

Compact near infrared sources in the center of the extraordinary galaxy IC 860

J. S. Gallagher^{1,2}, L. Schisgal¹, G. C. Privon^{3,4,5}, S. Aalto⁶, S. König⁶, R. Kotulla², J. Mangum³, W. St. John¹, D. Rigopoulou^{7,8}, and K. Alatalo^{9,10}

¹ Department of Physics and Astronomy, Macalester College, 1600 Grand Ave, St. Paul, MN 55438 USA
e-mail: jgallag1@macalester.edu

² Department of Astronomy, University of Wisconsin-Madison, 475 N. Charter St., Madison, WI 53706 USA

³ National Radio Astronomy Observatory, Edgemont Rd. Charlottesville, VA 22903 USA

⁴ Department of Astronomy, University of Florida, P.O. Box 112055, Gainesville, FL 32611 USA

⁵ Department of Astronomy, University of Virginia, P.O. Box 400325, Charlottesville, VA 22904 USA

⁶ Department of Space, Earth and Environment, Onsala Space Observatory, Chalmers University of Technology, 43992 Onsala, Sweden

⁷ Department of Physics, University of Oxford, Keble Road, Oxford OX1 3RH, UK

⁸ School of Sciences, European University Cyprus, Diogenes street, Engomi, 1516 Nicosia, Cyprus

⁹ Space Telescope Science Institute, 3700 San Martin Drive, Baltimore, MD 21218, USA

¹⁰ William H. Miller III Department of Physics and Astronomy, Johns Hopkins University, Baltimore, MD 21218, USA

Received

ABSTRACT

Context. Hubble Space Telescope (HST) images are used to study the structure of the central regions of the luminous infrared galaxy (LIRG) IC 860. IC 860 is of special interest as a system with an extreme central concentration of molecular gas cloaking its compact obscured nucleus (CON). The CON provides most of the $1.5 \times 10^{11} L_{\odot}$ luminosity in IC 860 from an undetermined combination of stellar and AGN power sources.

Aims. We mapped and photometered the central molecular zone (CMZ) of IC 860 motivated by a previous detection of a luminous compact nuclear source. Our objective was to study properties of the CMZ and its relationship to the CON, that we identified as an opaque central region in archival near infrared (NIR) images.

Methods. We measured the coordinates of the compact NIR source, IC860-a, from HST coordinates calibrated with Gaia positions. Photometry of the HST images yielded magnitudes, colors, and high V-band dust optical depths based on foreground screen dust models. Photometry corrected for dimming by dust yielded NIR luminosities of IC860-a and the CMZ.

Results. IC 860 has distinct compact central luminosity sources: Most of the NIR luminosity is from the CMZ while the LIRG-CON is an obscured region centered in the CMZ. IC860-a, in the northeast side of the CMZ, is offset by $\approx 0.2''$ from the CON, has a luminosity of $\sim 10^9 L_{\odot}$, and may be a massive young stellar complex or intruding nucleus.

Conclusions. The inner CMZ in IC 860 contains two luminous compact objects: The CON is identified for the first time as an obscured central source while the structure of the CMZ+CON is complicated by the presence of the IC860-a compact object, possibly a massive young stellar system or second nucleus. The presence of IC 860-a in combination with the CON is a further signature of the unusual evolution of the gas-rich IC 860 CMZ.

Key words. galaxies–evolution–nuclei–interactions

1. Introduction

IC 860 is an SBa galaxy located at a distance of 59 Mpc. Its unusual nature was noticed when Schmelz et al. (1986) detected 18 cm OH absorption. Soon thereafter IC 860 was recognized to be a luminous infrared galaxy (LIRG) (Soifer et al. 1987; Carico et al. 1988), Mirabel & Sanders (1988) found an unusual global HI 21 cm line in absorption, and Kazes et al. (1988) set a path for future studies by describing IC 860 as a “most peculiar galaxy”. Condon et al. (1990) found that a compact central radio source is present with a size of $<0.5''$. The intrinsic nature of this galaxy and its sources of infrared luminosity, however, remained unclear, but most investigators considered it to either be a non-interacting galaxy or a possible product of a minor merger (see discussions in Baan et al. 2017; Luo et al. 2022). IC 860 also has been classified as a post-burst galaxy with large scale

optical emission from shocks that suggest the presence of an AGN which is yet to be confirmed (Alatalo et al. 2016; Luo et al. 2022, and Figure 1).

Initial interferometric millimeter observations with modest angular resolution did not reveal the presence of a powerful nucleus in IC 860 (e.g., Imanishi 2006), but showed an inner molecular disk (e.g., see Alatalo et al. 2024, and references therein). Mid-infrared spectroscopy of the center of IC 860 with the *Spitzer Space Telescope* and radio observations of ammonia lines, however, detected absorption from molecules located in dense, hot molecular matter, demonstrating that unusual conditions exist (Lahuis et al. 2007; Mangum et al. 2013). Signatures in the form of maser emission and outflows further suggested that an obscured source of central activity existed as discussed by e.g., Baan & Klöckner (2006), who also provided evidence for the presence of heavy dust obscuration towards compact

sources in the center of IC 860 with their sub-arcsec radio continuum imaging. Subsequent high angular resolution observations with mm/submm interferometers established that the nucleus of IC 860 is its primary luminosity source. The nucleus is a compact highly obscured nucleus (CON).

CONs are defined as compact galaxy nuclei displaying vibrational HCN submillimeter emission lines arising in dusty, dense, warm interstellar matter that envelopes the nuclei (see Aalto 2013; Falstad et al. 2021). CONs also can be distinguished by their extreme opacities (Donnan et al. 2023) and mid-infrared spectral characteristics (García-Bernete et al. 2025). The radius of a CON is set by wavelength dependent dust opacity which is low in the millimeter. The existence of CONs demonstrates that galaxies in the current epoch can collect substantial amounts of low angular momentum molecular gas close to their nuclei. This low angular momentum gas has the potential to fuel rapid growth of nuclear regions, such as nuclear star clusters and central massive black holes (e.g., Cen 2015; Volonteri et al. 2015; Anglés-Alcázar et al. 2017; Ramos Almeida & Ricci 2017; Hickox & Alexander 2018; Gorski et al. 2024; Nishimura et al. 2024; Kritos & Silk 2026). That CONs make use of this fuel can be seen from their presence primarily in systems with $L_{FIR} \geq 10^{11} L_{\odot}$ where they are the major power sources in their LIRG hosts (Falstad et al. 2021; Nishimura et al. 2024). Unfortunately, the extreme optical depths in CONs hide the interior power sources from the X-ray to millimeter bands. Possible sources of energy include active nuclei, starbursts, or accretion luminosity from gas infalling to the CON, or likely some combination of these (e.g., Gorski et al. 2023).

Before the IC 860 CON was discovered, observations by Alonso-Herrero et al. (2006) with the Near Infrared Camera and Multi-Object Spectrometer 2 (NICMOS2; NIC2) on the Hubble Space telescope (HST) showed a point source nucleus candidate in IC 860 that is visible in the near-infrared. However, the absolute position of this source, IC860-a in this paper, was not known and therefore its relationship to the CON that was discovered later was not explored. Here we revisit the properties of the central regions of IC 860 with an emphasis on properties of the CON and IC860-a. Our study benefits from the access to archival high angular resolution images obtained with the HST. Improved coordinate reference frames based on stellar positions and motions from Gaia in Wide Field Camera 3 (WFC3) HST images now allow us to match positions from HST images to those obtained with mm/submm interferometers at sub-arcsecond levels.

The objective of this study is to provide an HST context for JWST observations of the center of IC 860 obtained in program JWST GO-01991, P.I. G. Privon. In the next section we review the archival HST observations that provide the data for our study and for the first time reveal the presence of an opaque CON in the NIR. Properties of the CMZ and inner 300 pc are considered in §3. The coordinates of IC860-a are tabulated in §4 and compared with those of the CON, which establishes that IC860-a is not the CON. Section 5 presents photometry from WFC3 and NIC2 images. Section 6 considers the levels of central dust obscuration in IC 860 derived from optical–NIR color maps. The dust corrected photometry leads to lower bound estimates for source luminosities. We discuss the results in §7 and give our conclusions in §8.

2. Observations

Our study is based on HST archival optical and near-infrared (NIR) images of IC 860 obtained with the WFC3¹. An overview of IC 860 from the HST imaging is shown in Figure 1. This system has well-defined spiral arms and a linear bar, consistent with its SBa morphological type.

The high intensity central region, shown by the contour in Figure 1, is prominent in the NIR but does not stand out in optical images. The gas-rich nature of the center of IC 860, however, can be seen in the form of extensive dust features to the west side of the galaxy’s center. This pattern indicates that dusty gas is above the galaxy’s mid-plane and only appears in absorption when observed against the stellar disk. Dusty extraplanar gas on the west side is below the disk and not detectable in absorption. The region within the inner contour in Figure 1 and to the west of the inner extraplanar dust features is the target of our investigation.

Photometric and initial source position measurements were obtained from the reduced fits images with corrections for charge transfer inefficiencies (fits “drc” file types) provided by the Mikulski Archive for Space Telescopes (MAST). Photometric calibration came from parameters in the image headers using standard techniques to convert the data count rates per pixel to magnitudes and fluxes. Initial position measurements were made using image coordinates included with the MAST data that we finalized by re-reducing one image.

3. Overview of central structures

The center of IC 860 is obscured by dust in optical bands (see Figure 1 and Luo et al. (2022)) but emerges in NIR images. Figure 2 shows the high surface brightness center of the oval region marked in Figure 1 (lower) in NIC2 NIR images. The inner annulus of the CMZ contains a zone of enhanced surface brightness with a major axis of 1.2'' and a minor axis of $\approx 0.4''$ ($340 \times 90 \text{ pc}^2$). The major axis is at PA=18°, aligned with the bar of IC 860. Longer wavelengths minimize the influence of dust obscuration on the central morphology. The central zone of enhanced surface brightness corresponds to molecular emission exterior to the CON (Aalto et al. 2015; Baan et al. 2017; Luo et al. 2022; Alatalo et al. 2024) and we identify it with the central molecular zone (CMZ) of IC 860.

The NIC2 images show the inner part of the CMZ as a luminous curved arc with the IC860-a appearing as a compact source near its northeastern edge. They have the advantage of small pixels at the cost of a reduced field of view relative to the WFC3/IR channel. The $R_{submm} \sim 10 \text{ pc}$ ($R_{obs} \approx 0.03''$) in IC860 determined from sub-millimeter molecular line and dust emission and the cm-wavelength radio continuum defines the position of the inner, high density core of the CON’s interstellar envelope that has a mass of $\leq 10^8 M_{\odot}$ (Aalto et al. 2015, 2019; González-Alfonso & Sakamoto 2019; Falstad et al. 2021). The radius of the dark, obscured region at the position of the CON is $\sim 1 \text{ pixel} = 0.075''$ (20 pc) in NIC2 NIR images. This marks the position of the opaque envelope that we assign to the outer surface of the spheroidal CON. Dust lanes faintly detected in the NIC2 F110W image connect to the area enclosed by the CMZ arc, the location of the CON (see §4 below), and are found

¹ HST Archival WFC3 images are from programs GO-10169 P. I. Alonso-Herrero (NIC2); datasets n8z13010-040 and GO-14715, P.I. K. Alatalo (WFC3); dataset id8n0101, id8n02010-030, id801q9Q, and id8n02wpq retrieved from the Mikulski Archive for Space Telescopes

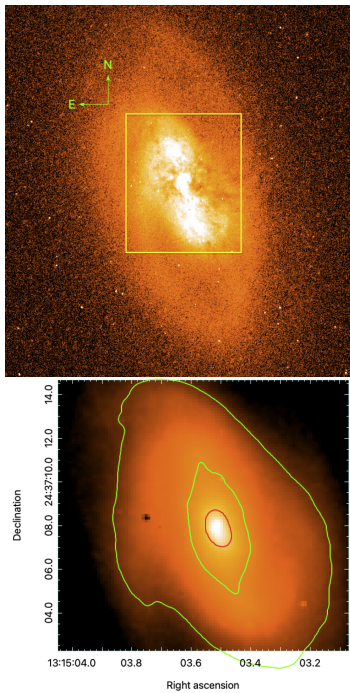


Fig. 1. *Upper:* HST WFC3/UVIS F438W blue light image of IC 860 showing the asymmetric dominant spiral arms and inner star-forming bar with a bright but dusty center. Luo et al. (2022) suggest the strong single arm is a possible signature of a past interaction. The $15 \times 15''^2$ (4.3×4.3 kpc 2) box defines the region shown in the lower image. The central dust lanes extending on the west side of center are typical of extraplanar material emanating from the position of the CON and its immediate surroundings (see Figures 6). The bright spots along the major axis appear to be regions of low obscuration, possibly containing younger stars in an inner bar structure. *Lower:* Central region of IC 860 from the WFC3/IR F140W observation of the boxed region in the upper figure. Isophotes are included to outline the structure of the inner galaxy while the central red contour delineates the high infrared surface brightness CMZ of IC 860 that contains the IC860-a compact source and is the location of its centrally concentrated CO 1-0 emission (Alatalo et al. 2024).

around the location of IC860-a. This pattern suggests the presence of organized gas flows in the central regions of IC 860 as discussed by Gorski et al. (2023). The CON is the source of a strong and likely dusty molecular wind which we do not consider when discussing the CON opacity. This issue needs to be explored with better data.

4. Position of the IC860-a compact source

Our objective in measuring the position of the IC860-a NIR source is to determine its location relative to that of the CON. The CON's coordinates are accurately known from a combination of radio continuum and molecular line observations (e.g., Aalto et al. 2019). IC860-a is detected in F814W and longer wavelength filters (see Figure 3). We searched for IC860-a by comparing archival WFC3 optical and NIR images with the NIC2 images and established that it is the point source measured by (Alonso-Herrero et al. 2006). Our initial reconnaissance also showed IC860-a to be at the same position in WFC3 filters ranging from F814W to F160W. The absence of IC860-a in the F606W and F475W WFC3 images reflects the high levels of dust obscuration deduced by Alonso-Herrero *et al.*, which was further confirmed by our analysis (see § 6).

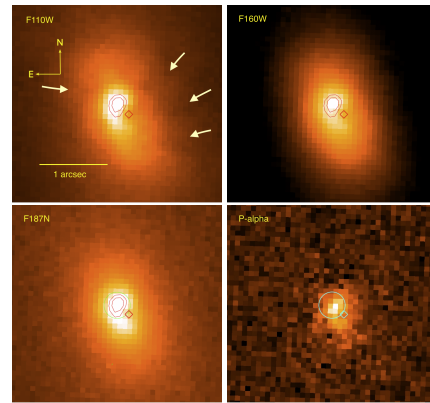


Fig. 2. Archival NIC2 images of the center of IC 860. The arc of enhanced surface brightness outlining the CMZ and the IC860-a source (contours) and the CON absorption region (diamond) are the main NIR features within this zone. Dust absorption clouds (arrows) are faintly visible in the F110W image as darker regions around IC860-a and the position of the CON. The F187N is a continuum band at IC 860's redshift. The CON appears as a dark source in the continuum images indicating a high NIR optical depth. The Pa α image includes a circle at the position of IC860-a and shows H-recombination emission from much of the CMZ. Coordinates are not included since the NIC2 data reference frames have coordinate offsets.

We first measured positions for IC860-a in the WFC3 F814W, F140W, and F160W images using the MAST-supplied coordinate frames using the IRAF task *radprof*. This tool plots intensity and of the region in multiple radial cuts and derives the location of the intensity peak and its positional error in pixel coordinates. The results showed IC860-a to have a well defined intensity profile above the complex background, especially in the NIR filters and that the peak position is consistent in position in the HST filters. Two archival F140W observations of IC 860 were obtained 6.5 months apart with different orientations and positions on the detector but yielded the same coordinates for IC860-a. Due to the small field of view we could not obtain the position of IC860-a from the NIC2 images.

Although the F814W image offers the advantage of the best angular resolution the effects of dust limit the quality of our measurements of the source location and flux. We chose the WFC3/IR F140W id8n01q9q image to determine our adopted position of IC860-a. This filter combines reasonable angular resolution and reduced sensitivity to dust. Coordinates for the F140W image were updated with positions from the Gaia DR3 catalog matched to stars in the field of view. In so doing we omitted one star in the Gaia catalog that lacked a proper motion measurement since this star therefore had an uncertain position at the time of the F140W observation, and also dealt with issues associated with bright stars. The image also was redrizzled to a $0.04''$ pixel scale as shown in Figure 3 and the IC860-a photocentroid fit with IRAF task *radprof* using a range in region sizes. The results were reproducible at the 0.5 pixel ($0.02''$) level in each coordinate for a total positional uncertainty for IC860-a of $\pm 0.03''$.

Our adopted position for IC860-a from updated coordinates in the F140W image is J2000 13:15:03.515 \pm 0.002, +24:37:07.96 \pm 0.02, which significantly differs from the IC 860 CON's position of J2000 13:15:03.506 +24:37:07.82 that has a total uncertainty of $0.02''$ (Aalto et al. 2019). IC860-a is offset $0.16 \pm 0.034''$ (≈ 50 pc in projection) to the north-northeast of the CON in IC 860. *The CON in IC 860 is not coincident with IC860-a; these are distinct structures.* As shown in Figure 3,

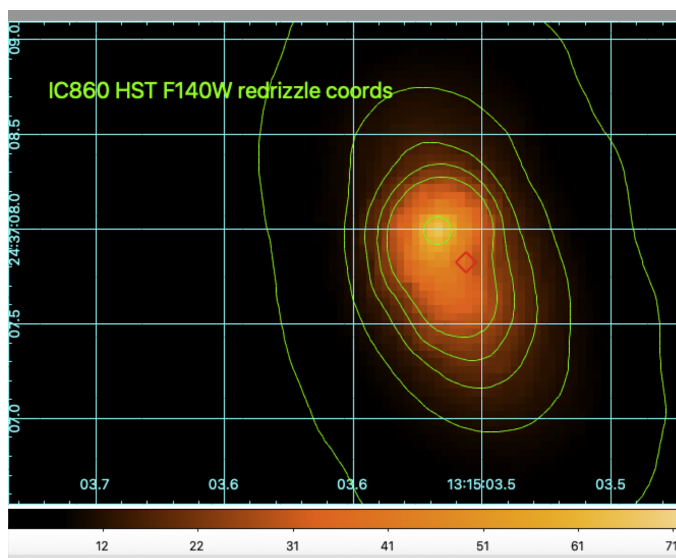


Fig. 3. WFC3 F140W image of the inner IC 860 CMZ region with updated J2000 FK5 coordinates. Locations of the IC860-a (yellow circle) and CON (red diamond) are displayed in this WFC3 F140W image of IC 860.

Table 1. IC 860 central structure positions

Object	RA	DEC
<i>CON</i> ^a	13:15:03.506	24:37:07.812
IC860-a adopted ^b	13:15:03.515±0.002	24:37:07.96±0.02
IC860-a, F814W ^c	13:15:03.514	24:37:07.96
IC860-a Dust ^d	13:15:03.517±0.002	24:37:07.80±0.02

Notes. Positions are J2000 ICRS derived from the WFC3 images as discussed in the text and below. *Notes:* (a) CON position from Aalto et al. (2019) Table 3 with a positional uncertainty of $\pm 0.02''$; (b) Position from re-reduced F140W image in this paper; (c) From archival image coordinate frame, uncertainty not well determined due to dust obscuration impact on the profile; (d) IC860-a reddening peak position measured from our optical depth maps (see Figure 6).

the CON is located at the inner edge of the curved CMZ structure and at the base of the central dusty region extending to the west that may mark a dusty wind. We measured the position of this opaque region in the NIC2 F110W image relative to that of IC860-a and determined that its location agrees with that of the CON. This position places the CON near the center of the CMZ, consistent with its status as the nucleus of IC 860. Skipper & Browne (2018) found that the radio source associated with the CON is possibly slightly displaced from the SDSS measurement of the isophotal center of IC 860, but our HST imaging with the updated coordinate frames confirms that the radio position of the CON is close to the center of the CMZ. A summary of our position measurements for IC860-a are in Table 1.

5. Photometry

5.1. IC 860a

For photometry of IC860-a we first removed the wider galaxy background by subtracting data smoothed by medians of 7×7 , 9×9 and 15×15 pixel² for WFC3/UVIS, WFC3/IR/ and NIC2 images, respectively. IC860-a was located and photometered using a combination of aperture photometry and the IRAF radprof

task to isolate the intensity peak and determine the peak intensity relative to the background. With this information we adopted an aperture with $r_{ap} = 0.15''$ that corresponds to the approximate level where IC 860-a merges into the CMZ background. Count rates and fluxes for all filters were derived using information in the image headers and standard HST magnitude calibrations.

No intensity maximum is visible at the location of IC860-a in the F606W image, and the surrounding regions are brighter than the position of IC860-a. We estimated a conservative lower limit $m(606)_{AB,IC860-a} \gtrsim 22.4$ by assuming the upper limit flux is equal to the square root of the mean count rate in a $0.15''$ radius aperture.

Following this approach we obtained $m(814)_{AB,IC860-a} \simeq 21.5$ and the source FWHM=5.8 pixels (65 pc). The F814W IC860-a source profile is larger than the diffraction limit, noisy, possibly slightly resolved, and likely significantly affected by dust absorption. Assuming an intrinsically red color of $(m(606)-m(814))_{0,AB} = 0.6$ for IC860-a leads to the lowest amount of dust reddening of $E(m(606)-m(814))_{AB} > 1.6$ for $A_\lambda \propto \lambda^{-0.7}$. This is an extreme lower limit stemming from uncertainties in the point source photometry as shown by our dust ratio measurement in §6 and NIR photometry by Alonso-Herrero et al. (2006).

NIR archival images of IC-860 are available from NIC2 and WFC3/IR observations. The smaller pixel scale of the NIC2 images better sample the HST PSF and are the choice for NIR photometry of the compact IC860-a source. The WFC3/IR data are more sensitive and have a wider field of view that is essential for position measurements as discussed above. We found that photometry from NIC2 and WFC3/NIR agrees to within 0.1 mag in the F160W filter (see §5.2 below). Flux measurements of IC860-a are not as well determined from the WFC3/NIR data as from NIC2 due to the difference in pixel sampling, but the agreement between the NIC2 and WFC3 F160W photometry shows that IC860-a has varied by $\lesssim 0.1$ mag during the 12.4 yr interval between these two observations. IC860-a is not a rapidly varying transient source such as a supernova.

Infrared photometry of IC860-a faces difficulties with backgrounds similar to those in the optical bands. In our approach the photometric uncertainty is based on the counts within the half maximum intensity radius. We do not include possible additional offsets due to aperture corrections as we make the conservative assumption that IC860-a contains an uncertain amount of emission from the CMZ arc. Thus our fluxes and magnitudes refer to IC860-a plus a contribution from the CMZ, i.e. the total emission within the half width diameter of IC860-a.

We carried out 2 pixel radius ($r=0.25''$) aperture photometry on the IC860-a in the WFC3/IR F140W and F160W images. We took advantage of the capabilities provided by the IRAF radprof task to carry out centered photometry with radial plots to determine the adopted backgrounds. IC860-a is cleanly detected in the archival WFC3/IR F140W and F160W images and has a FWHM of 3.8 pixels in the F140W filter, slightly larger than a pure point source. Although the background is noisy, the photometry is repeatable at the 20% level based on flux changes from small centering offsets. We calculated luminosities for IC860-a for $D=59$ Mpc and assuming $\tau_V=3.5$ and $\tau_\lambda \propto \lambda^{-0.7}$. To estimate the total luminosity we converted the absolute magnitudes to solar luminosities by comparing with the in-band AB absolute magnitudes of the Sun. Our preferred results come from the NIC2 F160W observation giving $L(IC860-a) \geq 8 \times 10^8 L_\odot$. This is a lower limit in that our aperture did not include the full intensity profile and the total extinction is uncertain. F160W WFC3/IR photometry with an $r=0.26''$ (2 pixel) aperture gives $L(IC860-a)_{bol} \lesssim 2 \times 10^9 L_\odot$. This is a strong upper limit due to

Table 2. IC860-a photometry

Filter	m_{AB}	A_λ	$\log(L/L_\odot)$
F606W ^a	$>23.6\pm 0.3$	≥ 3.5	>7.5
F814W ^b	≥ 21.5	≥ 2.7	≥ 7.8
F110W ^c	19.1	≥ 2.1	≥ 8.6
F140W ^d	17.9	≥ 1.6	≥ 8.9
F160W ^c	17.0	≥ 1.7	≥ 9.0

Notes. Photometry with $r=0.15''$ apertures with estimated uncertainty of ± 0.2 mag. Aperture corrections are not included. ^a Upper limit as IC860-a is not detected. ^b Data are shown as upper bounds on the observed magnitude due to modest contrast with the surroundings. This leads to lower bounds on the luminosity due to the use of the foreground screen model in combination with high optical depths. ^c Based on NIC2 images; F160W was used to estimate the luminosity of IC860-a; see text for discussion. ^d F140W data from WFC3/IR.

the poorer image sampling that leads to inclusion of more of the CMZ. Luminosities also depend on the quality of the foreground dust correction model, which is an additional source of uncertainty but generally leads to underestimates of fluxes and thus luminosities (see Gallagher et al. 2024, and the discussion below). We therefore adopt $L(\text{IC860-a})_{bol} \approx 10^{9\pm 0.3} L_\odot$, in agreement with the results found by (Alonso-Herrero et al. 2006) who derived $M(160)_{vega} = -19.6$ corresponding to $L(160)_{\text{IC860-a}} = 1.5 \times 10^9 L_\odot$. The results of the photometry are summarized in Table 2.

A second approach to find $L(\text{IC860-a})_{bol}$ comes from measurements of the in-band flux for each filter. Here we used the photometry key words from the headers. Our most reliable results are from the better sampled NIC2 images that give in-band luminosities per filter of $\sim 10\%$ of $L_{\text{IC860-a,bol}}$. The HST imaging data thus require that $L_{\text{IC860-a,bol}} \gg 10^8 L_\odot$.

The increasing luminosity of IC860-a with increasing wavelength in Table 2 is symptomatic of the limitations of the foreground screen model which become less severe when optical depths decrease at longer wavelengths. The optical color ratio data in the next section also suggest that we are not dealing with a system with an ideal foreground dust screen. This because IC860-a is both heavily reddened and has a substantial F814W surface brightness, a situation that is not expected for a foreground screen dust model because high opacities leading to strong reddening also require low source intensities. If dust and luminosity sources are mixed, then highly opaque systems will emit an intensity set by the source function. The source function for pure absorption in a homogeneous medium is $S_\lambda = j_\lambda/\kappa_\lambda$. Here j_λ is the volume emissivity that may rise into the NIR and κ_λ is the opacity that declines with increasing λ . In this situation, unlike the foreground screen prediction, S_λ from a very optically thick system can have a significantly reddened spectral energy distribution relative to the j_λ sources in combination with a substantial emergent intensity. The foreground screen model then provides a strict lower bound to the optical depths and dust obscuration corrections and our luminosities also are lower limits. In the case of IC860-a, derived luminosities are converging in the NIR, implying that the foreground screen model may be more realistic for interpreting the F160W data, but to be conservative we tabulate all of the IC860-a luminosities as lower limits.

5.2. The IC 860 CMZ

We selected the approximately elliptical central surface brightness region of $\sim 1.2'' \times 0.4''$ in IC 860 based on the location of rapid outwards decrease in the brightnesses of isophotes to define the CMZ that is centered on the CO 1-0 distribution (Alatalo et al. 2024). CMZ fluxes from the pair of WFC3 F140W observations separated by 6.5 months and with different HST orientations agree to within 1%. We measured the observed flux ratio between the CMZ and IC860-a and found that IC860-a contributes $\approx 10\%$ of the total F160W flux from the CMZ. Since IC860-a appears to be more heavily obscured than the CMZ, the observed flux fraction is a lower limit to the true luminosity ratio. The results from CMZ photometry are summarized in Table 3 that gives an observed F160W mean CMZ intensity of $\mu_H = 14.4$ magnitudes $''^{-2}$ and a luminosity density of $\approx 5 \times 10^{10} L_\odot \text{ kpc}^2$. The observed μ_H is near the upper bound for early-type galaxies (e.g., Wu et al. 2005). Radio continuum measurements show little flux from the CMZ aside from the area of the CON (Condon et al. 1990; Baan et al. 2017; Aalto et al. 2019). Pa α emission from the CMZ may be a sign of active star formation outside of the CON so long as the emission is locally produced by young, massive stars. This issue requires further exploration that is beyond the scope of this study.

The molecular ISM-rich CMZ that is luminous in the NIR surrounds the CON. In IC 860 the CON is a central peak above a relatively smooth, larger-scale radial gradient in the density of interstellar matter. The absence of NIR emission from the CON requires that the distribution of its luminosity sources relative to dusty gas differs in a major way from that in the CMZ. The source function in the CMZ leads to substantial NIR intensities while the CON is not detected. We can understand this change if most luminosity sources in the CON are located behind a $\tau_{NIR} >$ several dust screen. Figure 4 is a cartoon model of the $R \lesssim 100$ pc center of the IC 860 CMZ based on our qualitative analysis.

A Pa α emission line map (Figure 2, lower right corner) was made by scaling the NIC2 F187N filter image as an off band to subtract the continuum from the F190N image that fortunately contains the Pa α emission line (see Figure 2). The peak of the Pa α emission is slightly offset from the F190N continuum peak of IC860-a with the Pa α emission being more spatially extended than the NIR continuum. Alonso-Herrero et al. (2006) interpreted the presence of Pa α emission along much of the arc as evidence for the presence of young massive stars within the CMZ and IC860-a. However, we have yet to determine whether the Pa α emission is due to stellar photoionization. We defer a discussion of properties of emission lines and possible levels of associated star forming activity in the IC 860 CMZ to the analysis of JWST spectra obtained in program JWST GO-01991, P. I. G. Privon that can better constrain its properties (Privon *et al.* in preparation).

6. Central dust obscuration

Dust features in the center of IC 860 dominate its optical appearance as shown in Figure 1 (see Luo et al. (2022) for discussions of the larger scale dust distribution). We produced the dust visual optical depth map of IC 860 in Figure 6 from the ratio of count rates in the F606W to those in the F814W WFC3 images. Optical depths are derived under the assumption of a purely absorbing foreground dust screen following the methodology based on image ratios as compared to low obscuration regions as described by Gallagher et al. (2024) and Schisgal et al. (2025). As in these previous studies, we adopt a power law form for the long wave-

Table 3. IC860-a CMZ infrared photometry

Filter	m_{AB}	A_{λ}^a	$\log(L/L_{\odot}^b)$
WF3-F140W	15.4	≥ 1.4	~ 9.8
WF3-F160W	15.2	≥ 1.3	~ 9.8
NI-F160W	15.3	≥ 1.3	~ 9.8

Notes. CMZ defined by photometry with the isophote shown in Figure 1 corresponding to $\mu_{AB}=16.6 \text{ mag}''^2$ in the WFC3 F140W filter. ^aForeground screen extinction scaled from an assumed mean $\tau_V=2.5$ for the CMZ (see §6 below). ^bLuminosity based on the tabulated A_{λ} . As discussed in §6, similar luminosities in the NIR suggests the foreground screen approximation is providing reasonable results.

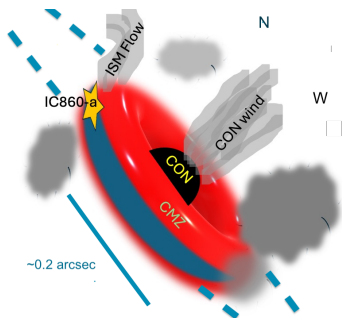


Fig. 4. Conceptual cartoon view of the inner 100 pc of the IC 860 CMZ as observed in the NIR. The CON, spherical in this idealization, is opaque in the NIR while the inner, high brightness annular zone of the CMZ is illuminated with a peak intensity near its edge. In this part of the CMZ a mixture of stars and dust leads to a combination of substantial reddening and high intensity in the NIR. This situation does not prevail at the optically thick surface of the CON that we observe. The sharp edge of the inner CMZ in this cartoon is not physical. Dashed lines show that the CMZ extends well beyond the illustrated central region. The NIR intensity and foreground optical depth estimates peak at the position of IC860-a, an indication that dust is associated with IC860-a. The area to the right (west) of the CON has higher levels of dust obscuration, likely due to dusty outflows. Dust structures with moderately high opacity around IC860-a and elsewhere are suggestive of additional gas flows.

length obscuration, $\tau_{\lambda} = \tau_V(\lambda/550 \text{ nm})^{-0.7}$. This technique² provides lower limits to the calculated optical depths presented in Figure 6.

Figure 5 shows the central dust structure based on the optical depths derived with foreground screen models. In this idealized model dust is only distributed exterior to the area of study, including the location of the CON. Since the CON is opaque at the wavelengths of the HST observations, it does not contribute to color maps. Therefore the opacity estimate from the foreground dust screen model is not affected by the CON. As previously discussed by Luo et al. (2022), most of the IC 860 CMZ is highly obscured with $\tau_V \geq 2$. The dust absorption mainly extends to the west, approximately perpendicular to the major axis of IC 860. The high opacity central dust screen in IC 860 is best understood as originating from out-of-plane gas flows, consistent with observations of central molecular flows (e.g., Aalto et al. 2015; Luo et al. 2022; Gorski et al. 2023). Central regions of enhanced brightness visible in the F438W data in Figure 1 have bluer colors than their surroundings. They are likely to be areas with young stars observed through patches of low dust obscuration.

² Note that Alonso-Herrero et al. (2006) used a power law with an exponent of -0.8

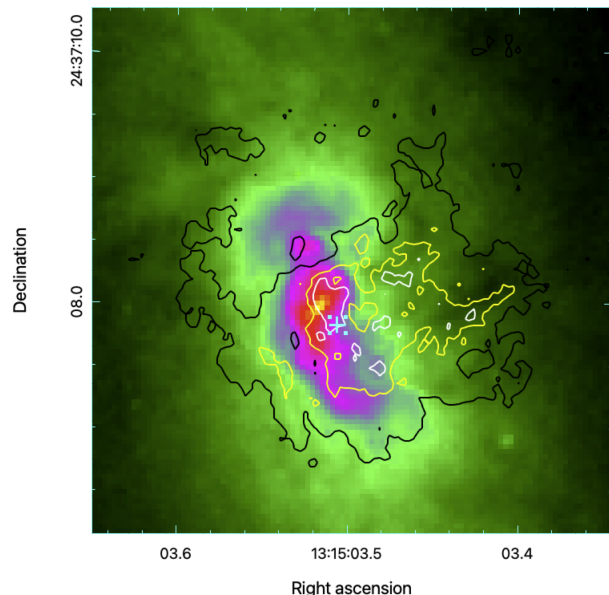


Fig. 5. False color version of the F814W image of the center of IC 860 showing the brightness distribution with foreground τ_V contours superimposed. Contour levels for τ_V are white=3.5 (region A), yellow=3.0 (region B), and black=2.0 (region C). Very substantial reddening is present across the $\sim 3 \times 10^5 \text{ pc}^2$ central region. The cross marks the location of the CON. The distribution of dust extending above the disk of IC 860 shows that outflows occur across the CMZ, similar to the situation in the CON-host Zw 049.057 (Gallagher et al. 2024).

However, we did not model these regions since they do not align with either the CMZ or IC 860-a that are the focus of this study.

An outstanding feature of our HST F606W–F814W flux-ratio color map is the compact high opacity feature that is coincident with the IC860-a and offset from the location of the CON. As we discussed in §5, detection of the IC860-a in the F814W image and its absence in the F606W image naturally leads to the structure of the associated compact, deep dust absorption feature that is only slightly more extended than the F814W point spread function. We photometered IC860-a in the color-ratio image with an $r=0.079''$ (2 pixel) circular aperture corresponding to a diameter of approximately 40 pc. We adopted $I_{F606W}/I_{F814W}=1.65 \pm 0.05$ for the unobscured galaxy background color-ratio taken from the surrounding regions with low dust obscuration. Our aperture photometry yielded a formal foreground screen dust opacity estimate for IC860-a of $\tau_V \geq 3.5 \pm 0.5$ within the 2 pixel radius aperture. As shown in Figure 6 this reddening maximum is within the larger dust complex B that extends over much of the central region of IC 860. Although measurements of $\tau_V > 3$ are necessarily uncertain (as well as being lower limits), our HST V-I color ratio map indicates that IC860-a is substantially more deeply obscured than its surroundings and likely contains dust.

The highly dust obscured CON is located near the southern edge of the opacity region A in Figure 6, a location that is not unique in terms of τ_V . Archival HST images of IC 860 provide the first detection of a CON through its deep NIR absorption. HST NIR and optical observations of the centers of the CON-LIRGs NGC 4418 and Zw 049.057 do not detect the CONs as discrete sources of emission or absorption (Scoville et al. 2000; Gallagher et al. 2024; Schisgal et al. 2025). In these galaxies and in IC 860 the CONs are not in locations where the foreground shows signs of unusually high optical depths. However, in IC 860 we find the CON as an NIR dark absorption feature that

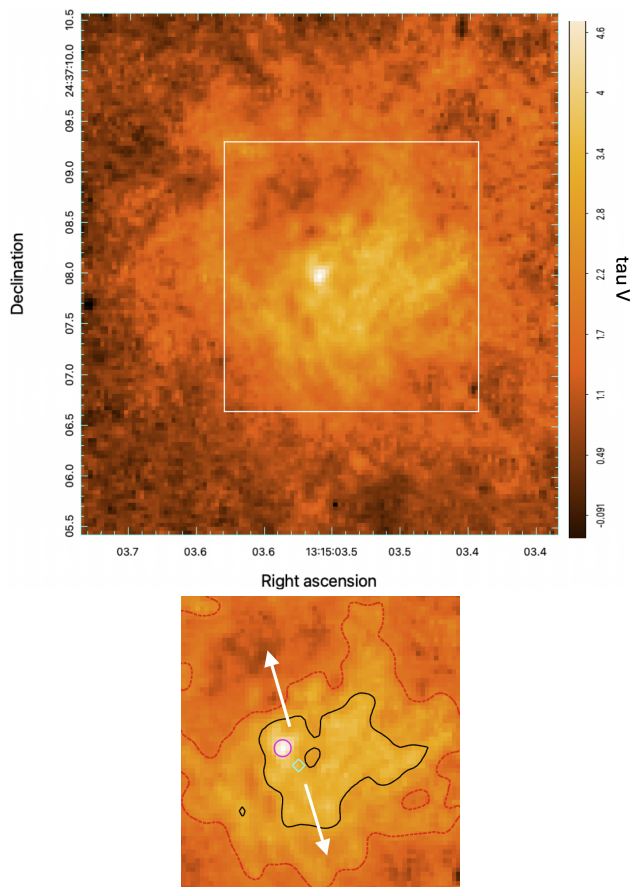


Fig. 6. *Upper* Estimated V-band optical depths in the central region of IC 860 from the $m(606) - m(814)$ HST color relative to the blue circumnuclear color of $m(606) - m(f814) = -0.3$. *Lower* Zoom in on the CMZ in the 2.5×2.7 arcsec² (0.7×0.8 kpc²) area shown by the white box. The dashed red contour is for $\tau_V = 2.0$ and the black contour marks $\tau_V = 3.0$. A circle marks IC860-a, the diamond is at the position of the CON, and the arrows point along the major axis of the CMZ.

is not significantly reddened. As discussed by Gallagher et al. (2024), this combination of features shows that high opacity originates within the CON rather than arising in more extensive, less dense foreground screen of interstellar matter.

Our observed ~ 20 pc radius of the NIR absorption from the IC 860 CON that is ≥ 2 times the R_{submm} follows the pattern expected from the radiative transfer model by González-Alfonso & Sakamoto (2019) for IC 860. This model adopts a spherical structure, radius of 28 pc, gas column of $N(\text{H}) \approx 10^{25} \text{ cm}^{-2}$, inward, radially increasing dust densities, and either young stars or AGN as luminosity sources. It predicts, as we observed, that the submm CON “core” is embedded in a somewhat larger envelope of dense interstellar matter. We adopted a spheroidal CON model for this paper (see eq(1) below) as the simplest option, an assumption that needs to be confirmed.

7. Discussion

7.1. The IC 860 nuclear region

The two compact central luminosity sources in IC 860 contribute in distinct ways to the central luminosity of the galaxy. Our analysis in combination with the Alonso-Herrero et al. (2006) study prove that IC860-a and the CMZ produce the central region’s

NIR luminosity while the CON dominates in the total luminosity in the far-IR. This combination of wavelength-dependent contributions complicates previous interpretations of the mid-IR spectra of IC 860. In optical-bands dust absorption reduces the visibility of the CMZ and the central luminosity is from a more spatially extended, diffuse collection emission islands probably due to patchy dust screening in combination with local regions of recent formation (see Figure 1 and (Luo et al. 2022)).

As a result, the properties derived for the center of IC 860 are strongly dependent on the wavelength coverage and angular resolution of the observations. For example, Lahuis et al. (2007) analyzed Spitzer Space Telescope (SST) mid-infrared spectra of IC 860 taken with a $4.7''$ width slit. The SST instrumental point spread function in the 14 micron region of interest was expected to be $3.5''$. The SST spectrograph slit therefore encompassed the entire CMZ and its immediate surroundings, sampling emission from the CMZ, IC860-a, and extended nuclear region as well as any mid-infrared emission from the CON.

7.2. Masses

The presence of an additional compact source in the center of IC 860 raises questions about its relationship, if any, to the CON. Is the IC 860 CON an unusual example of a galaxy nucleus or could it be an extreme version of a star forming molecular cloud as in the case of the Medusa galaxy (König et al. 2014)? However, the CON is at the centroid velocity of IC 860, is at the center of the CMZ, is surrounded by rotating gas disks with regular structures with velocity fields that are aligned in position angle with the main stellar disk, and is the radio continuum point source (Baan et al. 2017; Aalto et al. 2019; Luo et al. 2022). These properties are consistent with expectations for the IC 860 nucleus.

In principle, the total nuclear mass also can distinguish between these two scenarios for the nature of the CON. In a young star-forming cloud with the normal low star formation efficiency, the total mass will be close to that of the molecular medium. A CON should also include substantial mass contributions from preexisting stars and likely a central supermassive black hole. We also would normally expect the mass of the nucleus of IC 860 to exceed that of any compact circumnuclear stellar complexes that form in the CMZ.

7.3. Mass of the CON

Unfortunately, dynamical mass estimates for the IC 860 CON are difficult to obtain (e.g., due to uncertainties in orientation and internal dynamics) and range between $2 \times 10^7 M_{\odot}$ and $\leq 9 \times 10^7 M_{\odot}$ within $R = 10$ pc depending on the inclination of the rotating component of molecular gas within the CON (Aalto et al. 2019). We preferred the higher CON mass that assumes an inclination of 60° that fits with the flattening observed for the CMZ. The molecular mass in the CON can be crudely estimated by assuming a spheroidal distribution of interstellar matter with radius R_{dust} corresponding to the assumed column density N_{H} ,

$$M_{\text{ISM}}/M_{\odot} \sim 4 \times 10^7 M_{\odot} (N_{\text{H}} / (10^{25} \text{ cm}^{-2} (R_{\text{dust}} / 20 \text{ pc})^2 \epsilon_{\text{CON}}) \quad (1)$$

where $\epsilon_{\text{CON}} \leq 1.0$ is a parameter to account for possible the flattening of the CON’s gaseous envelope.

The significant optical depth at $R_{\text{NIR}} \sim 20$ pc absorption edge of the CON only provides a weak limit of $N_{\text{H}}(20 \text{ pc}) \geq 10^{22} \text{ cm}^{-2}$ so the $N(\text{H})$ of the CON is driven by the molecular line results which are model dependent. For this

study we adopted $N_H = 10^{25} \text{ cm}^{-2}$ from the greenhouse models by González-Alfonso & Sakamoto (2019). Aalto et al. (2019) give a FWHM radius of 10 pc while the NIC2 observations, as discussed in §3, suggest a radius $R_{dust} \approx 20$ pc for the high NIR opacity outer limit of the CON that we adopted to estimate the total dynamical mass of the CON. Aalto et al. (2019) also find the molecular CON is rotating with a $\sigma/V_{rot} \approx 0.5$ implying that the CON in reality has a rotationally flattened structure so that $\epsilon_{CON} < 1$. Our data lack the resolution to determine if the CON is flattened at $R_{dust} = 20$ pc. Therefore we simply extrapolated the (Aalto et al. 2019) dynamical model to the CON mass enclosed within 20 pc with a constant V_{rot} that gives $M_{dyn} \sim 2 \times 10^8 M_\odot$ with a significant fraction of its mass in the form of gas under the assumption that ϵ_{CON} is not small.

This combination of parameters, despite their considerable uncertainty, limits the stellar + central black hole mass within $R_{NIR} \approx 20$ pc containing the CON to $< 10^8 M_\odot$. Refining mass measurements for the CON will provide an important constraint on the nature of the underlying nuclear region. Nuclear star clusters and their surroundings in the $10^7 - 10^8 M_\odot$ mass range primarily are found in late-type spirals (e.g., Kormendy & McClure 1993; Barth et al. 2009; Georgiev et al. 2016). The Milky Way galaxy with $(\log(M_\star) \approx 10^{10.8} M_\odot)$ offers a point of comparison. The mass within a radius of 20 pc from the Milky Way's nucleus is $\sim 5 \times 10^7 M_\odot$ (e.g., Feldmeier-Krause et al. 2025). Thus if the Milky Way were to add the gas cloak of a CON, we would expect its total mass to be $\sim 10^8 M_\odot$, similar to the situation in IC 860. However, the uncertainties in the mass of the IC 860 CON are too large to establish whether the CON is a heavily dust obscured version of a normal galaxy nucleus.

7.4. Mass of IC860-a

The mass of IC860-a can be estimated from its luminosity by adopting a stellar model and making an assumption about the nature of this source. In considering the possibility that it is a galaxy nucleus, we assume that IC860-a is not a radio-quiet AGN based on its lack of X-ray emission (Luo et al. 2022). We derive a stellar mass for a nucleus model assuming an old stellar population mass-to-light of $\gamma_{160} = 1.0$ and that the central black hole makes a minor contribution to the mass within $R \approx 30$ pc. For a young stellar complex model we take $\gamma_{160} = 0.3$ that would normally be associated with an actively star-forming system. A significantly lower value of γ_{160} requires an unusual bottom-light or top-heavy stellar initial mass function. The mass of IC860-a for a stellar model with a Kroupa-type initial mass function is

$$M_{IC860-a,*} \approx 3 \times 10^8 (L_{IC860-a,bol} / 10^9 L_\odot) (\gamma_{160} / 0.3) M_\odot. \quad (2)$$

Given the concentration of molecular gas in the center of IC 860, a young massive star forming complex with a radius of about 30 pc in principle could explain IC860-a. However, the photometric mass of $M_{IC860-a,*} \sim 10^8 M_\odot$ is extremely high for a compact star forming region. While the mass of such a young region could be reduced by the presence of additional light contributions from a path through the CMZ, a young stellar explanation for IC860-a requires an unusual event. A further complication arises in that the mass for a young stellar complex model for IC 860-a is potentially similar to the mass estimated for the IC 860 CON. If IC860-a is a young stellar complex, then its presence would demonstrate that star formation can be a significant gas sink within the CMZ that competes with the CON for interstellar material.

A different possibility is that IC860-a is an inactive nucleus, a remainder from a possible past merger (see discussion

of a merger in Luo et al. 2022). This option leads to some concerns but cannot be excluded with the present data. For a nucleus, eq.(2) with $\gamma_{160} = 1.0$ leads to an inferred stellar mass of $\geq 10^9 M_\odot$ for IC860-a which could exceed the mass within the same radius of the CON. The lack of any dynamical anomalies in the CO 1-0 velocity field at the position of IC860-a (Luo et al. 2022; Alatalo et al. 2024) may be an indication that IC860-a is substantially less massive than the CMZ. Our mass estimate for a second nucleus is $\sim 10-20\%$ of the $\sim 10^{10} M_\odot$ mass of the CMZ, suggesting that a second nucleus within the CMZ without a clear dynamical signal might be feasible. Dynamical modeling is required to determine if the mass ratio between an IC86-a nucleus and CMZ is sufficiently small to avoid detectable perturbations of the outer CMZ CO disk kinematics. This difficulty could be avoided if IC860-a were a nucleus located out of the plane of the IC 860 CMZ, but its heavy dust extinction then is problematic. The possibility that IC860-a is behind the galaxy, seen through the dusty edge of the CMZ, is inconsistent with the JWST detection of mid-infrared thermal from dust associated with IC 860-a (Privon *et al.* in preparation). More sensitive measurements of the structure and kinematics of the CON, IC860-a, and the CMZ are needed to constrain the properties of this complex region.

8. Conclusions

The LIRG IC 860 contains a pair of compact, luminous central sources: The CON is observed as an opaque central region in the NIR but provides the bulk of the system's luminosity that emerges in the far infrared. IC 860-a is a compact, prominent NIR source with properties consistent with either a massive young stellar complex or second galaxy nucleus. Both of these features are located at projected positions within the CMZ.

- This is the first identification of a CON as a compact, opaque feature in the NIR. The NIR extent of absorption due to the CON is approximately 20 pc, ≥ 2 times the radius of the CON as a submillimeter source. As we discussed in §6, the observed radius based on a spheroidal CON is in reasonable agreement with greenhouse CON models having an $N(H)$ column similar to the observed values for IC 860, consistent with the presence of a massive envelope of low angular momentum gas. The opacity and lack of highly reddened emission from the CON in the NIR indicate that its power sources lie behind a dust layer that is substantially optically thick at the $2 m\mu$ long wavelength limit of the HST data.
- We analyzed the compact NIR source, IC860-a that originally was identified by Alonso-Herrero et al. (2006) as the IC 860 nucleus. We confirm their finding that it is heavily obscured by dust with $\tau_V \geq 3.5$. We found that IC860-a is offset by ≈ 50 pc ($0.16 \pm 0.03''$) in projection from the IC 860 CON that is at the expected location of the IC 860 nucleus. This result is supported by the off-center position of IC860-a in the CMZ and the position of the CON corresponding to the deeply obscured center of the CMZ. IC 860 therefore contains two luminous central compact sources. IC 860-a, with $L \sim 10^9 L_\odot$ that has not varied significantly over 12.4 yr and makes a modest contribution to the central NIR luminosity while the CON provides the bulk of the $\sim 10^{11} L_\odot$ total power radiated from IC 860.
- The inner $R \leq 100$ pc in the center of IC 860 is blanketed by a complex distribution of extraplanar dust with optical depths of $\tau_V \geq 2$. Our dust opacities are based on foreground screen models which can lead to underestimates of the true obscuration levels and thus lower bounds for luminosities based on

photometric measurements. The extensive presence of dust exterior to the galaxy's mid-plane illustrates the importance of large scale gas flows in the center of IC 860. The existence of the extended interstellar medium traced by dust absorption is consistent with molecular line evidence for gas flows, and especially the detection of outflows and inflows associated with the CON.

- An approximately ellipsoidal region of enhanced NIR surface brightness with a ~ 500 pc major axis coexists with the central disk of molecular gas with a ~ 500 pc major axis in the IC 860 CMZ. This region has a disk morphology and is aligned with and centered on the star forming main stellar bar in IC 860 that is a potential source of inflowing gas.
- The innermost part of the CMZ has the properties of an inclined disk-like region with a radius of ~ 60 pc. Its brighter edge is inclined towards us with an $R_{dust} \approx 20$ pc deeply obscured core at the location of the CON. $\text{Pa}\alpha$ emission is present along the rim of the region indicating that ionization sources, uncertain in nature but possibly young stars, are associated with the optically thick CMZ.
- Our photometric data give a stellar mass for IC860-a of $\geq 10^{8-9} M_{\odot}$. The lower mass range for IC860-a is similar to dynamical mass estimates for the IC 860 CON of $\sim 10^8 M_{\odot}$ within $R=20$ pc, which is typical of a moderate mass galaxy nucleus. IC 860-a presents interpretive difficulties due to its uncertain properties. If IC860-a is an intruding second nucleus, then its mass equals or exceeds that of the CON nucleus. This introduces issues stemming from the lack of evidence for perturbations of the observed regular kinematics of nearby molecular gas in the CMZ. If IC860-a is a young stellar complex, then its inferred mass of $\sim 10^8 M_{\odot}$, is unusually high and possibly comparable to the mass of the CON. The nature of this unusual object and its impact on the evolution of the CMZ and CON remain to be determined.
- The presence of two massive compact objects in the center of IC 860 within a 50 pc projected distance adds to the complexity of the inner CMZ. A second nucleus would be suggestive of a ULIRG-like CON formation process involving nucleus-nucleus interactions. The presence of a massive young stellar complex could indicate that the CON has had significant competition for obtaining gas from the CMZ. If IC860-a is a young stellar complex, then both it and the CON are products of the extremely gas-rich environment which is accessible to more detailed studies. Better determinations of the properties of IC860-a, the CON, and the kinematics of the inner CMZ are essential for modeling the current conditions and evolution of IC 860 and its CON.

References

- Aalto, S. 2013, in IAU Symposium, Vol. 292, Molecular Gas, Dust, and Star Formation in Galaxies, ed. T. Wong & J. Ott, 199–208
- Aalto, S., Martín, S., Costagliola, F., et al. 2015, *A&A*, 584, A42
- Aalto, S., Müller, S., König, S., et al. 2019, *A&A*, 627, A147
- Alatalo, K., Lisenfeld, U., Lanz, L., et al. 2016, *ApJ*, 827, 106
- Alatalo, K., Petric, A. O., Lanz, L., et al. 2024, *ApJ*, 975, 241
- Alonso-Herrero, A., Rieke, G. H., Rieke, M. J., et al. 2006, *ApJ*, 650, 835
- Anglés-Alcázar, D., Davé, R., Faucher-Giguère, C.-A., Özel, F., & Hopkins, P. F. 2017, *MNRAS*, 464, 2840
- Baan, W. A., An, T., Klöckner, H.-R., & Thomasson, P. 2017, *MNRAS*, 469, 916
- Baan, W. A. & Klöckner, H. R. 2006, *A&A*, 449, 559
- Barth, A. J., Strigari, L. E., Bentz, M. C., Greene, J. E., & Ho, L. C. 2009, *ApJ*, 690, 1031
- Carico, D. P., Sanders, D. B., Soifer, B. T., et al. 1988, *AJ*, 95, 356
- Cen, R. 2015, *ApJ*, 805, L9
- Condon, J. J., Helou, G., Sanders, D. B., & Soifer, B. T. 1990, *ApJS*, 73, 359
- Donnan, F. R., Rigopoulou, D., García-Berete, I., et al. 2023, *A&A*, 669, A87
- Falstad, N., Aalto, S., König, S., et al. 2021, *A&A*, 649, A105
- Feldmeier-Krause, A., Veršič, T., van de Ven, G., Gallego-Cano, E., & Neumayer, N. 2025, *A&A*, 699, A239
- Gallagher, J. S., Kotulla, R., Laufman, L., et al. 2024, *ApJS*, 274, 3
- García-Berete, I., Donnan, F. R., Rigopoulou, D., et al. 2025, *A&A*, 696, A135
- Georgiev, I. Y., Böker, T., Leigh, N., Lützgendorf, N., & Neumayer, N. 2016, *MNRAS*, 457, 2122
- González-Alfonso, E. & Sakamoto, K. 2019, *ApJ*, 882, 153
- Gorski, M. D., Aalto, S., König, S., et al. 2023, *A&A*, 670, A70
- Gorski, M. D., Aalto, S., König, S., et al. 2024, *A&A*, 684, L11
- Hickox, R. C. & Alexander, D. M. 2018, *ARA&A*, 56, 625
- Imanishi, M. 2006, *AJ*, 131, 2406
- Kazes, I., Karoji, H., Sofue, Y., Nakai, N., & Handa, T. 1988, *A&A*, 197, L22
- König, S., Aalto, S., Lindroos, L., et al. 2014, *A&A*, 569, A6
- Kormendy, J. & McClure, R. D. 1993, *AJ*, 105, 1793
- Kritos, K. & Silk, J. 2026, *ApJ*, 1000, L21
- Lahuis, F., Spoon, H. W. W., Tielens, A. G. G. M., et al. 2007, *ApJ*, 659, 296
- Luo, Y., Rowlands, K., Alatalo, K., et al. 2022, *ApJ*, 938, 63
- Mangum, J. G., Darling, J., Henkel, C., et al. 2013, *ApJ*, 779, 33
- Mirabel, I. F. & Sanders, D. B. 1988, *ApJ*, 335, 104
- Nishimura, Y., Aalto, S., Gorski, M. D., et al. 2024, *A&A*, 686, A48
- Ramos Almeida, C. & Ricci, C. 2017, *Nature Astronomy*, 1, 679
- Schisgal, L., Gallagher, J., John, W. S., & Krause, J. 2025, *Research Notes of the American Astronomical Society*, 9, 82
- Schmelz, J. T., Baan, W. A., Haschick, A. D., & Eder, J. 1986, *AJ*, 92, 1291
- Scoville, N. Z., Evans, A. S., Thompson, R., et al. 2000, *AJ*, 119, 991
- Skipper, C. J. & Browne, I. W. A. 2018, *MNRAS*, 475, 5179
- Soifer, B. T., Sanders, D. B., Madore, B. F., et al. 1987, *ApJ*, 320, 238
- Volonteri, M., Silk, J., & Dubus, G. 2015, *ApJ*, 804, 148
- Wu, H., Shao, Z., Mo, H. J., Xia, X., & Deng, Z. 2005, *ApJ*, 622, 244

Acknowledgements. Based on observations made with the NASA/ESA Hubble Space Telescope, and obtained from the Hubble Legacy Archive, which is a collaboration between the Space Telescope Science Institute (STScI/NASA), the Space Telescope European Coordinating Facility (ST-ECF/ESAC/ESA) and the Canadian Astronomy Data Centre (CADM/NRC/CSA). This study is associated with program JWST GO-01991. Support for this research as a part of program JWST GO-01991 was provided by NASA through a grant from the Space Telescope Science Institute, which is operated by the Association of Universities for Research in Astronomy, Inc., under NASA contract NAS 5-26555. The National Radio Astronomy Observatory and Green Bank Observatory are facilities of the U.S. National Science Foundation operated under cooperative agreement by Associated Universities, Inc. JG, LS, and WStJ thank Macalester College for providing computing resources for this research. We also express appreciation to STScI and the NICMOS and WFC3 instrument teams for providing the excellent archival observations of IC 860, the CON-quest team for the many fruitful discussions of CON properties, and Dr. Elena Sabbi for her advice on the procedures for assigning celestial coordinates to HST images. This paper was improved through consideration of issues identified in a constructive report by an anonymous referee. *Software:* SAOimage DS9, IRAF, Python